Carbohydrate Polymers 82 (2010) 54–61

Contents lists available at ScienceDirect

Carbohydrate Polymers

journal homepage: www.elsevier.com/locate/carbpol

Multi-scale morphological characterisation of flax: From the stem to the fibrils

K. Charlet [a,*], J.P. Jernot [a], S. Eve [a], M. Gomina [a], J. Bréard [b]

[a] Laboratoire de Cristallographie et Sciences des Matériaux, CRISMAT UMR 6508 ENSICAEN/CNRS, 6 Boulevard Maréchal Juin, 14050 Caen Cedex 4, France
[b] Laboratoire d'Ondes et Milieux Complexes, LOMC, Université du Havre, 53 rue de Prosny, 76058 Le Havre Cedex, France

ARTICLE INFO

Article history:
Received 26 January 2010
Received in revised form 10 April 2010
Accepted 13 April 2010
Available online 20 April 2010

Keywords:
Bundles
Fibres
Morphology
Focused ion beam
Mechanical properties

ABSTRACT

In this study, investigations were carried out on flax at different levels of observation. Stems, bundles and elementary fibres were studied in order to correctly understand the fibre structure and deformation so that the mechanical behaviour of derived flax fibre-based composite materials could be modelled. New structural information was obtained and correlated to mechanical properties. The main results are that fibres taken near the root are the largest of the stem, that both intra-bundle size variability and inter-fibre size scattering are linked to large intra-fibre size dispersion, that fibre mechanical properties should be calculated on the basis of their diameter near their rupture point rather than their mean diameter, and that a new schema of the fibre internal structure could be drawn from focused ion beam experiments.

1. Introduction

1.1. Flax fibres as reinforcement in composite materials

Flax fibres are more and more foreseen as potential alternatives to the synthetic E-glass fibres usually used to reinforce polymeric matrices: the low density and the relatively high stiffness of the former make them more competitive than the latter. The processing of more environmentally friendly composites, also called "eco-composites", requires a precise characterisation of the considered natural fibres, in order to understand their structure before modelling their deformation behaviour and predicting the resulting composite mechanical properties.

1.2. Flax fibres as a composite structure model

Flax can be described as a composite structure from the macroscopic scale to the nanoscopic scale (Fig. 1). The cross-section of a flax stem, which is roughly 80 cm long and 2 mm wide, reveals more or less dense concentric layers which either protect the material from outside attacks and confer rigidity to the stem (the bark) or allow water and nutritive substances to penetrate from the centre of the stem to the fibres (the xylem). Both the bark and the xylem are eliminated during the stages of retting and scutching.

On a smaller scale, bundles of fibres are composed of several elementary fibres glued together by a pectic cement; the partial separation of these bundles into smaller pieces (for example, during hackling) gives rise to what are generally called technical fibres, which contain from single numbers to tens of elementary fibres and can reach the same height as the flax stem.

Elementary flax fibres are 10–80 mm long with a diameter of 10–40 μm (Bossuyt, 1941; Rowell, Han, & Rowell, 2000). They can be described as the concentric association of 2 types of cell walls, the outer primary and the inner secondary, the latter also divided into 3 parts which differ in terms of thickness and structure. The fibre also possesses a central hole, called the lumen; during cell life it is filled by cytoplasm which disappears when the plant dies (i.e. during retting), leading to a more or less large hole.

Finally, at the nanoscopic scale, each cell wall consists of concentric lamellae a few nanometres thick. In each lamella, cellulose fibrils are embedded in an amorphous matrix mainly composed of pectins and hemicelluloses. These fibrils, which are few nanometres wide (Baley, 2002; Eichhorn et al., 2001; Fink, Hofmann, & Purz, 1990; Fujita & Harada, 1991; Hearle, 1962; Näslund, Vuong, Chanzy, & Jésior, 1988) and are well ordered in each lamella, represent the stiffest constituents of the fibre, with a theoretical Young's modulus of 137 GPa (Sakurada, Nukushina, & Ito, 1962). Both their quantity and their arrangement are likely to be responsible for the good mechanical properties of flax fibres (Charlet, 2008).

1.3. Outlines of the study

The aim of this study is to accurately describe flax morphology at different scales. First, stems were explored in order to highlight

* Corresponding author. Present address: IFMA/LaMI, Les Cézeaux BP 265, 63 175 Clermont Ferrand, France. Tel.: +33 473 288 139; fax: +33 473 288 027.
E-mail address: charlet.karine@free.fr (K. Charlet).

0144-8617/$ – see front matter © 2010 Elsevier Ltd. All rights reserved.
doi:10.1016/j.carbpol.2010.04.022

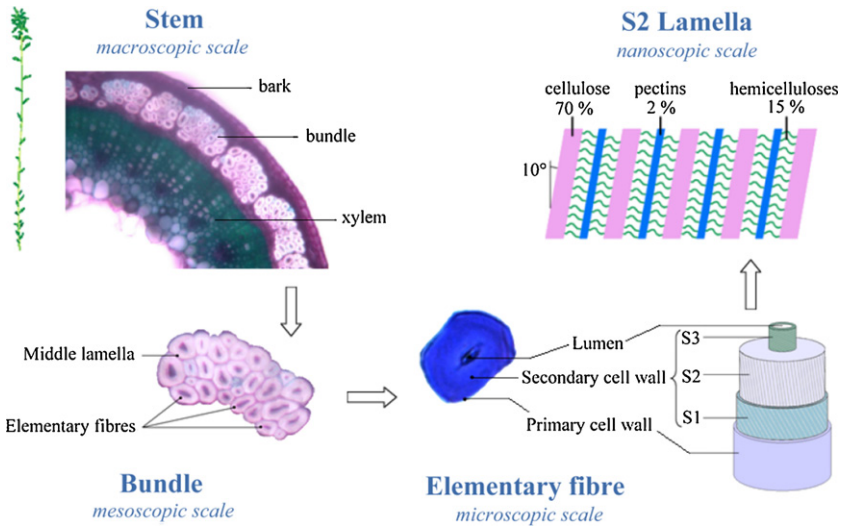

Fig. 1. Cross-sections and schematic representations of flax at different scales, from the stem to the cellulose fibrils.

the influence of the fibre position on its dimensions. Next, bundles were studied to determine the arrangement of the fibres composing them. Then hundreds of elementary fibres were measured, both transversely and longitudinally, to estimate their mean dimensions. Lastly, the cell walls constituting the fibres were observed and their thickness measured using a FIB microscope. At each level of observation, the structural parameters are correlated to mechanical properties in order to help to understand the deformation behaviour of each entity.

2. Materials and methods

Except for the exploration of flax stems, the results of only one variety of flax (Hermès) are given here. The stems were harvested in Normandy, France, in 2004 and supplied by Dehondt Technology.

2.1. Exploration of flax stems

Before retting, the length and the width of the stems at mid-length were measured and those whose dimensions were close to the mean (about 70 cm and 1.5 mm respectively) were selected (2 for the Hermès variety, 1 for the Agatha variety). Cross-sections were taken from the stem with a razor blade and carefully referenced. They were then bleached and treated with a substance (Mirande's reagent) which colours the cellulose red and the lignin green, making possible the distinction of each fibre.

With our method, cross-sections were taken every 5 cm along the stem, from the bottom to the top; for each bundle of each cross-section obtained, the surface area was measured and the number of fibres it contained was counted. This enabled differences in flax morphology according to the position along the stem to be highlighted, even if the bundles in the cross-sections taken from the highest part of the stems were more difficult to observe than those of the other parts, mainly due to their small size.

2.2. Study of stem cross-sections

An 18 mm long central part of a representative stem was sliced into around 70 consecutive 250 μm thick cross-sections, which were treated as mentioned above and observed. Eight bundles in which the fibres could easily be identified in a maximum number of consecutive cross-sections were selected. The surface areas of these bundles were determined and the number of fibres was counted for each cross-section, enabling the variation in bundle surface area and the mean equivalent fibre diameter over the selected part of the stem to be identified.

2.3. Microscopic analysis of fibre cross-sections

Fibres were extracted from stems in the traditional manner by retting, scutching and hackling (Weightman & Kindred, 2005). Then they were embedded longitudinally, in the form of long tows, in an epoxy resin, and cut transversally using a microtome. The 20 μm thick cross-sections obtained were stained with toluidine blue and observed using an optical transmission microscope.

The orientation of the tows was scrupulously noted in order to differentiate subsequently the fibres located at the top, at the bottom or in the middle of the stems. At least 500 fibres of each group were observed.

As the images obtained could not be automatically processed, an original program (Charlet, Morvan, Bréard, Jernot, & Gomina, 2006) was developed in order to obtain the dimensions of each fibre and of its lumen: their outlines were manually drawn using tracing paper; then the hundreds of ring shapes obtained were scanned and appropriate image analysis software enabled the estimation, for each cell, of the fibre and lumen surface area and perimeter. From these results, the equivalent fibre diameter (i.e. considering the fibre as a perfect disk) and the porosity (defined as the ratio of the lumen surface area to the fibre surface area) were then determined.

2.4. Longitudinal observation of flax fibres (SEM)

About 20 single fibres were manually extracted from long tows originating in the central part of several flax stems. For each fibre, its extremities were glued on a paper frame so that its width could be measured over almost all its length. This frame was then put into a SEM chamber (Hitachi S-3000N) without any coating. Micrographs were taken at regular intervals (from 500 μm to 2 mm) under a pressure of 25 Pa at a working distance of about 15 mm, an acceleration voltage of 15 kV and a magnification of 900, in order to obtain the diameter profile of each fibre.

2.5. Determination of the internal structure of fibres (FIB)

The internal structure of the fibres was studied using a FEI 200XP focused ion beam (FIB) microscope. In this system, gallium ions scan the sample in the same way as the electrons do in a SEM. Gallium ions ($Z = 31$) strongly interact with the flax fibre, releasing

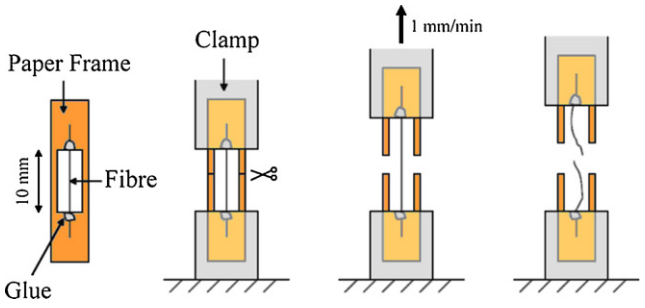

Fig. 2. Schematic representation of a flax fibre tensile test.

secondary ions and secondary electrons, which are used to capture an image of the sample surface. This method enables the different layers of a fibre to be revealed by destroying their interfaces (Domengès & Charlet, 2010). No prior embedment or cut of the fibre is needed, simplifying the sample manipulations compared, for example, to TEM experiments.

The protocol was as follows: an elementary fibre was taken from the tow and its extremities were glued to the metallic sample holder using silver paint. Prior to the FIB experiment, the fibre surface was protected with a thin Au–Pd layer deposited by evaporation. The holder was then placed within the FIB chamber. A first 0.2 μm thick Pt protective layer was deposited on the fibre surface over a large area and a second, thicker, Pt protective strap was positioned near the area of interest. The cross-section could then be etched with the beam perpendicularly to the fibre axis using a high-current ion beam. Finally, the holder was tilted at an angle of 45° and a secondary electron image of the fibre cross-section was obtained using a very low-current ion beam of a few picoamperes. Further scans of the fibre cross-section were performed, revealing some aspects of its inner structure.

2.6. Tensile testing of flax fibres

The mechanical properties of elementary flax fibres were determined by tensile tests (Fig. 2). Elementary fibres were glued on a brown paper frame so that the fibre was free over a length of 10 mm. The upper and lower sides of the frame were clamped to a MTS-type tensile testing machine equipped with a 10 N capacity load cell, and then the other sides were cut to free the fibre. Loading was applied to the fibre at a constant crosshead displacement rate of 1 mm/min until the fibre ruptured. Since strain could not be measured by using an extensometer, crosshead displacement was used to estimate deformation during the test. Stress was calculated as the force/cross-section ratio, the force being given by the load cell and the cross-section by the average of 5 measurements carried out along the fibre before the tensile test.

3. Results and discussion

3.1. Bundles of flax fibres

From the exploration of 3 flax stems, the number of fibres visible on each cross-section was counted and is shown in Fig. 3a as a function of the abscissa along the stem. Three different parts can be roughly identified according to these results: the bottom (about 20 cm long), the middle (about 40 cm long) and the top (about 20 cm long), although only one studied stem attained this last part, the other stem top bundles being too indistinct.

The measured total area of each bundle and number of fibres per cross-section allowed the mean fibre diameter to be calculated for each stem cross-section, in a first approach by considering the fibres as perfect disks. The variations in this mean fibre diameter are given in Fig. 3b as a function of the abscissa along the stem. It appeared that the mean diameter decreases from the bottom to the top of the stem, from 30 μm in the lowest part to about 18 μm in the middle and top parts. Thus, the middle part of the stem is not only the one that exhibits the largest number of fibres but also the one in which the thinnest fibres can be found.

3.2. "Technical" flax fibres

The variation in the quantity of fibres and the surface area of different bundles was determined from the investigation of successive cross-sections taken from the middle part of the stem. Eight of these bundles were clear enough to be easily distinguished and analysed over few millimetres. For each bundle, its surface was measured, the number of fibres was counted, and these results

Table 1
Mean surface area, amount of fibres and mean fibre diameter obtained from the exploration of 8 bundles over a middle section of a flax stem.

Bundle	Mean bundle surface area (μm²)	Amount of fibres per bundle	Mean fibre diameter (μm)
1	17,558 ± 2506	62 ± 8	19
2	9595 ± 1265	34 ± 3	19
3	13,973 ± 2761	44 ± 4	20
4	10,913 ± 1492	43 ± 4	18
5	6262 ± 1285	28 ± 3	17
6	17,938 ± 1871	57 ± 4	20
7	18,306 ± 2347	53 ± 5	21
8	16,509 ± 1921	48 ± 3	21

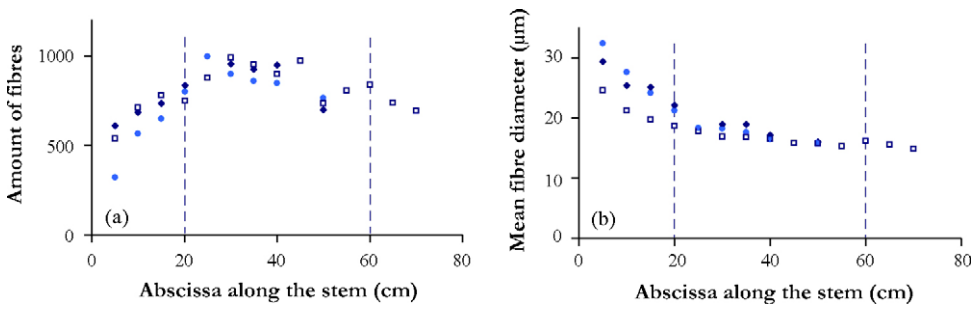

Fig. 3. Variation in quantity of fibres (a) and mean fibre diameter (b) along 3 flax stems.

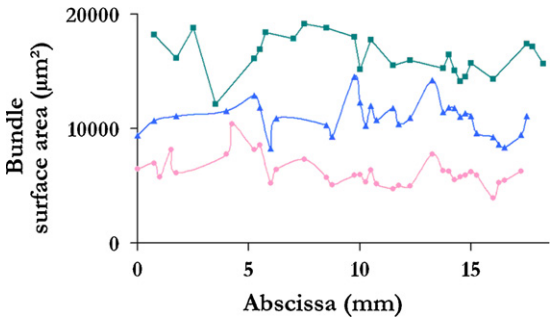

Fig. 4. Variation in surface area of 3 bundles along a 18 mm long stem section.

enabled a mean fibre diameter to be calculated, again considering the fibres as perfectly round. Table 1 gathers the data (average and standard deviation) measured, counted or calculated for each of these 8 bundles all along the selected part of the stem. For the sake of clarity, Fig. 4 presents the variation in surface area of only 3 of these analysed bundles as a function of the abscissa along the stem part.

The relative standard deviations around the mean surface area of each bundle range between 10% and 20%. This gives an indication of the size scattering of a bundle along its length, but does not indicate whether this scattering is due to a size variation of each of its fibres (intra-fibre size variability) or to the relative position of the fibres within the bundle (inter-fibre size variability). This requires the analysis of the size of single fibres, which is described in the next section.

The determination of the mechanical behaviour of the technical fibres, which are composed of different elementary flax fibres glued together by a pectic cement, is based on tensile tests carried out at different gauge lengths. The deformation of the flax bundle is expected to begin with local failures of this weak pectic interface (leading to fibre sliding), followed by the occurrence of microcracks on the fibre surface before the rupture of all elementary fibres (Romhány, Karger-Kocsis, & Czigány, 2003). According to Bos (2004), who tensile-tested flax bundles, mean strength (as well as strength scattering) decreases as gauge length increases, up to a value of about 500 MPa, which is reached as soon as the gauge length exceeds the mean elementary fibre length, i.e. roughly 20 mm (cf. section "Flax fibres as a composite structure model"). Below this length, fibre sliding is hindered, leading to higher (but more dispersed) values of strength, up to more than 1000 MPa.

Table 2
Results of the morphological analysis carried out on embedded fibres.

Position in the stem	Amount of fibres analysed	Mean diameter (µm)	Porosity (%)
Top	498	14 ± 4	3 ± 2
Middle	855	12 ± 3	3 ± 2
Bottom	903	17 ± 5	4 ± 2

This bundle effect prevents the mechanical properties of the technical flax fibres from reaching the values obtained by tensile testing elementary fibres (cf. section "Elementary flax fibres"). Thus, flax bundles are generally mechanically or chemically treated (hackling, carding ...) so as to eliminate the cement which keeps the elementary fibres glued together and to make them as fine as possible. Nevertheless, these treatments result in non-negligible damage (Bos, Van den Oever, & Peters, 2002), which reduces fibre strength. Thus, the strongest technical fibre is likely to be of medium size (both in length and width), in order to limit not only the damage undergone during treatment but also elementary fibre sliding during bundle deformation.

3.3. Elementary flax fibres

Transverse observations of flax fibres embedded in epoxy resin were made using an optical microscope (Fig. 5). Because of contrast issues (marks in the resin presenting the same grey shade as some fibres; fibres not well outlined, especially when considering blocks of fibres; fibres or lumens exhibiting different grey shades, making impossible the use of any colour threshold...), automatic measurement of the fibre dimensions was impossible. Thus, the size measurements (perimeter and surface area) of each fibre and lumen were made using a "home-made" method (Charlet et al., 2006). The results obtained on fibres taken in the three different parts of the stems are shown in Table 2: the diameter is calculated from the cross-section of the fibre, assuming a circular cross-section, and porosity is defined as the ratio between lumen surface area and fibre surface area.

The values of cell surface S and perimeter P, measured for the 2256 analysed fibres, enabled the estimation of a form factor f, defined as:

$$f = \frac{4\pi S}{P^2} \quad (1)$$

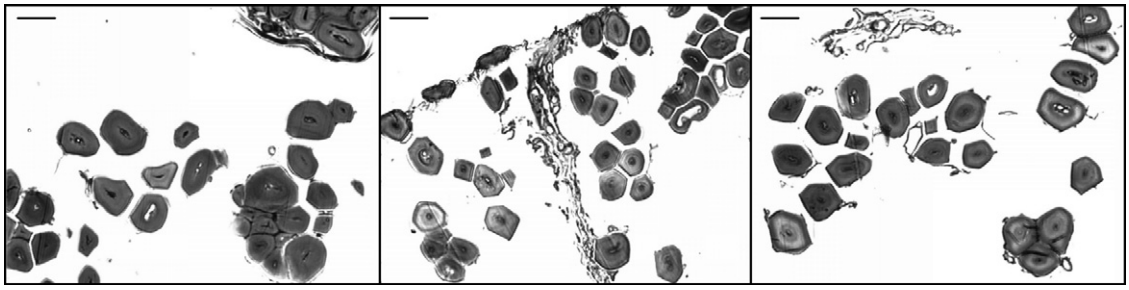

Fig. 5. Optical micrographs of transversely-cut flax fibres embedded in epoxy resin (the scale bars indicate 20 µm).

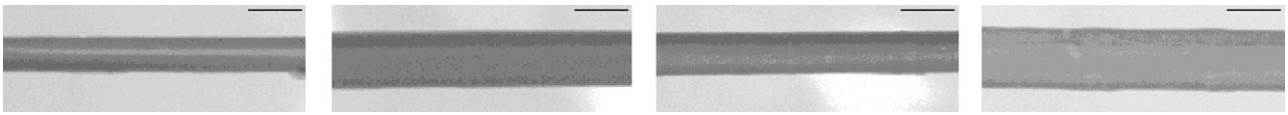

Fig. 6. SEM micrographs of an elementary flax fibre at different abscissas (1 mm, 7 mm, 9 mm and 14 mm respectively). The measured diameters on each micrograph are 13.0 µm, 20.8 µm, 15.3 µm and 22.5 µm respectively. The total length of the considered fibre is 15.6 mm and the mean diameter measured over its whole length is 16.5 ± 3.1 µm (the scale bars indicate 20 µm).

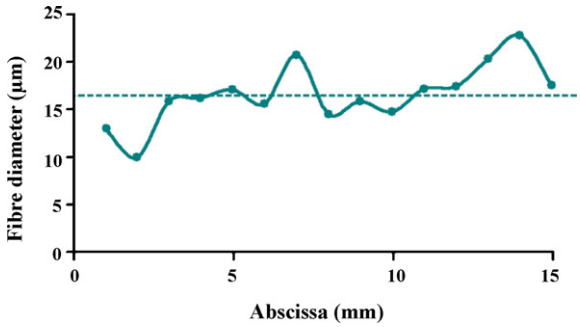

Fig. 7. Diameter profile of the single fibre illustrated in Fig. 6 along its whole length.

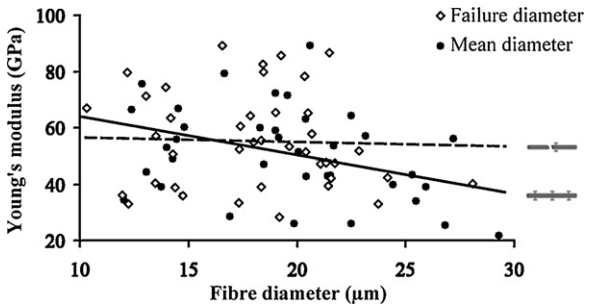

Fig. 8. Young's modulus as a function of either the diameter near the fibre failure point or the mean fibre diameter.

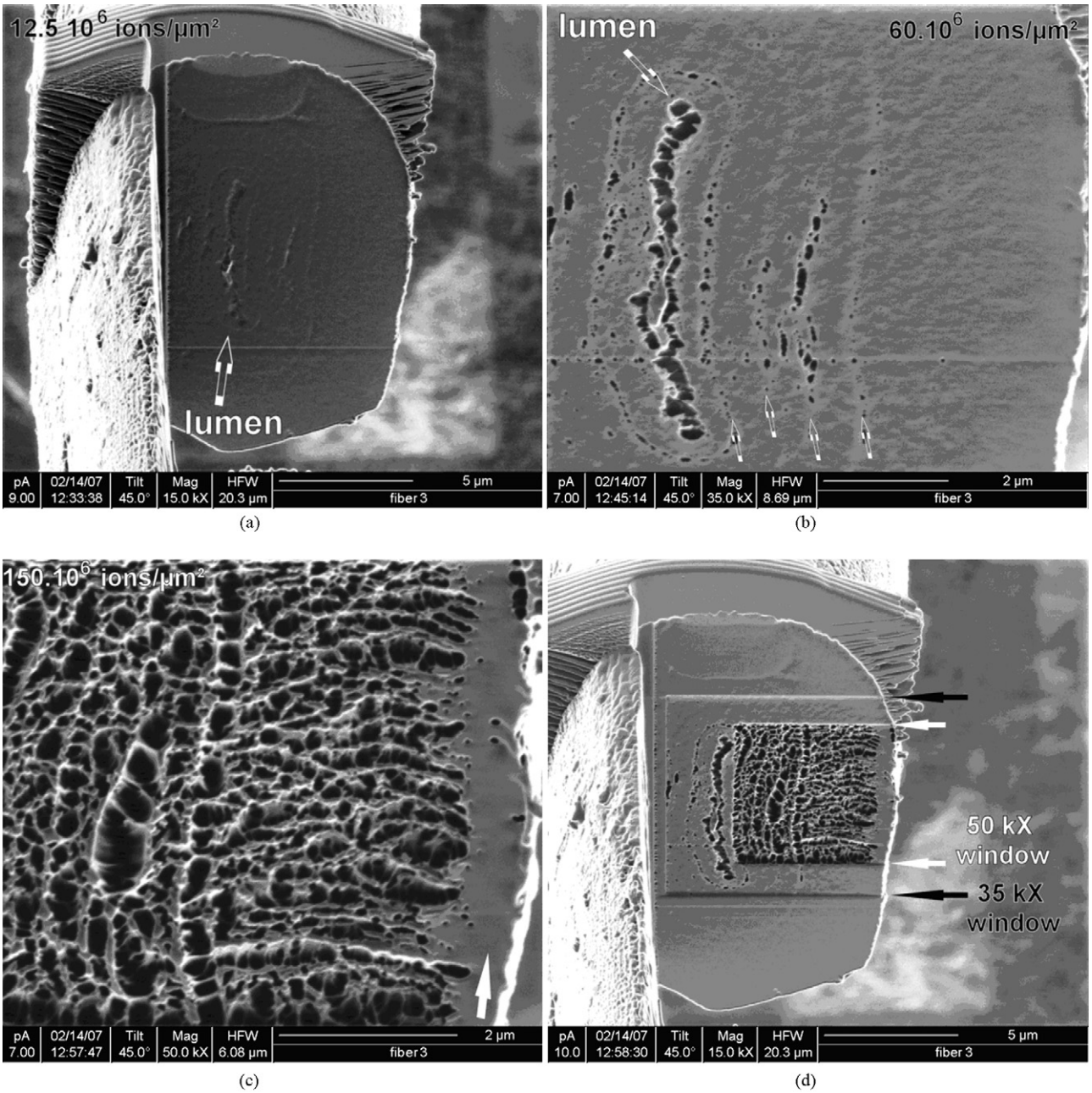

Fig. 9. Secondary electron FIB images of an elementary fiber cross-section, after (a) low, (b) medium and (c) high irradiation doses; (d) low-magnification image showing the different scanning windows used for this experiment.

This factor is equal to 1 for a round particle and 0 for a line. Here, the mean value for f is 0.9, which is comparable to the value obtained for a hexagon (f = 0.907). Nevertheless, Fig. 5 clearly shows that a hexagonal geometry is not a better approximation of the real fibre shape than a circular one. Moreover, the hypothesis of fibre circularity has the advantage of allowing an easier comparison of data among different species or different fibre locations, by using a calculated diameter as the main parameter; note that a comparison of surface areas would lead to the same conclusions. Finally, as described in the following, the dispersions of fibre dimensions and properties largely exceed the error generated by approximating the fibre shape as a circle; in fact the micrographs presented in Fig. 5 clearly show that there are more differences in size than in shape among the fibres.

From these results, the mean standard deviation around the mean fibre diameter can be estimated at 25–30%. Moreover, they show that the finest and the least porous fibres are located at the top and in the middle of the stem, which corresponds with the growth of the stem. The bottom fibres, which are the first to appear in the stem, grow slowly under relatively poor environmental conditions during April; thus their growth preferentially follows the radial direction rather than the longitudinal axis, leading to wide, short and hollow cells. On the contrary, the middle and top fibres develop more rapidly under sunnier weather conditions (May and June), both in the radial and the longitudinal directions, leading to longer, denser and thinner fibres.

Longitudinal observations of elementary fibres were also carried out to determine the variation in fibre diameter over almost its whole length (Fig. 6). An example of fibre diameter profile is given in Fig. 7. It shows that the diameter significantly varies all along the fibre, doubling in the space of a few millimetres.

According to the diameter profiles obtained for about 20 elementary fibres, the relative standard deviation around the mean diameter is approximately 20%. This value, which gives an indication of the scattering along a single fibre, must be compared with the relative standard deviation around the mean diameter obtained on a large population of fibres (25–30%). It may suggest that this latter scattering is due not only to size differences observed among several fibres but also (and rather) to the variation in diameter along each single fibre.

Concerning the organisation of fibres within a bundle, this analysis also suggests that fibre size variation conditions that of the bundle, since the standard deviation around the mean bundle area (10–20%) is lower than that around the mean fibre area (40%). "Intra-fibre size variability" is thus likely to be responsible for the bundle size variation.

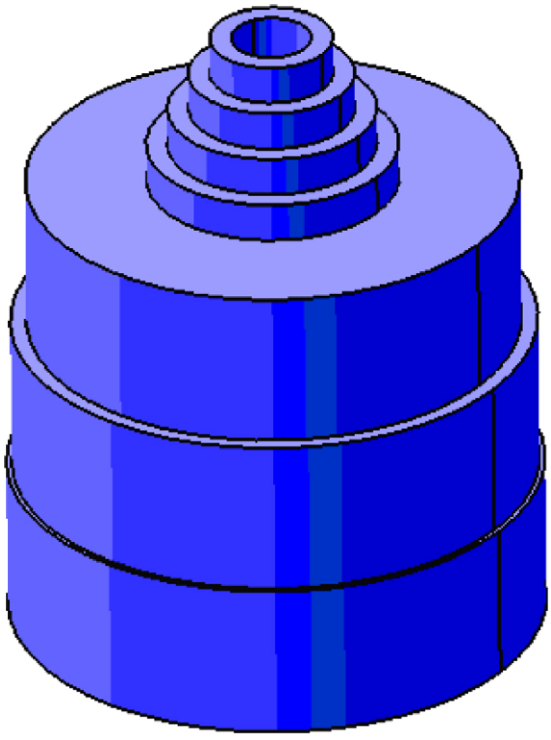

Fig. 10. Schematic representation of the flax fibre structure.

Another consequence of this large fibre dimension scattering is that it brings into question the notion of fibre diameter generally used to calculate the mechanical properties of fibres. Usually, a couple of images are taken along a single fibre in order to estimate a "mean fibre diameter". From the example given above (Figs. 6 and 7), it appears that this average value has no sense, since it strongly depends on the location of the measurements.

The mechanical properties of elementary flax fibres were studied by tensile testing. According to several authors (Baley, 2002;

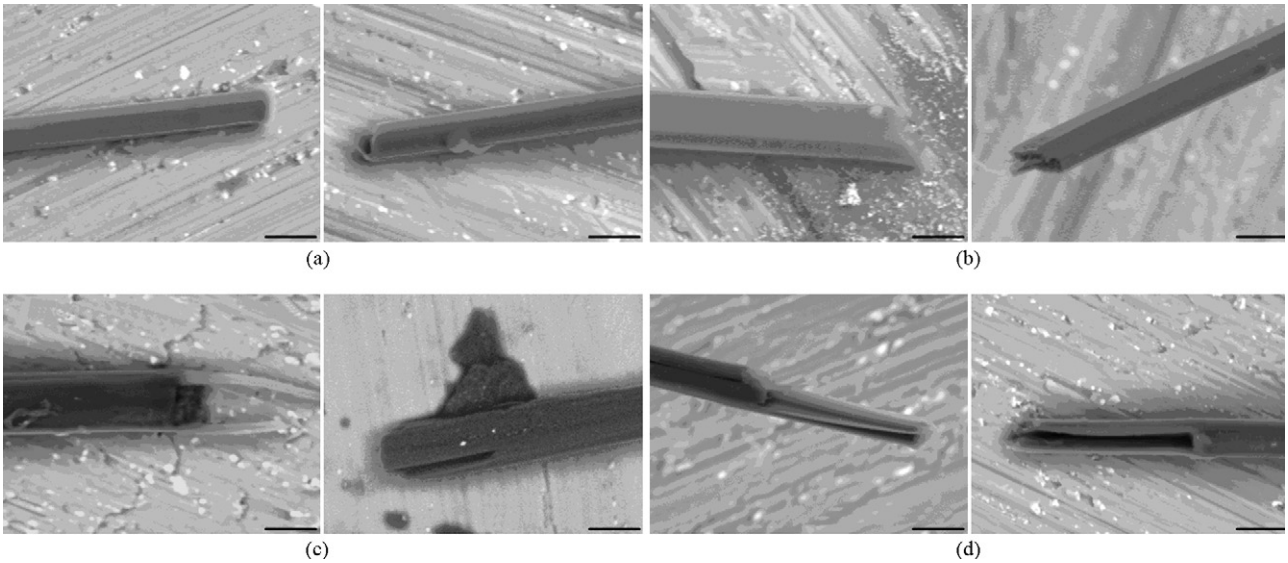

Fig. 11. SEM micrographs of 4 tensile-tested fibres near the rupture point: (a) and (b) exhibit preferentially the straight rupture mode, (c) and (d) the delamination rupture mode (the scale bars indicate 20 μm).

Batra, 1998; Beukers & Van Hinte, 1999; Davies & Bruce, 1998; Ganster & Fink, 1999; Troger, Wegener, & Seemann, 1998; Van den Oever et al., 2000), their mean strength is about 1200 MPa, their failure strain is around 2% and their mean Young's modulus reaches 60 GPa. The dependence of strength on fibre size has already been underlined in the literature and explained in terms of Weibull's statistics: the larger the fibre, the higher its probability of containing a defect and thus of failing prematurely compared to a smaller fibre (Andersons, Sparnins, Joffe, & Wallström, 2005; Zafeiropoulos & Baillie, 2007).

The fibre's Young's modulus presents the same dependency on size (though generally weakened by a rather large scattering of the values), but has never been clearly justified. Whereas strength is logically a function of sample size, Young's modulus is defined as an intrinsic parameter which should not vary with the sample dimensions. However, according to the previous paragraph, the definition of fibre dimensions is quite uncertain. An attempt was made to plot the variation in Young's modulus as a function of another dimensional parameter, fibre diameter close to the rupture point after a tensile test. Fig. 8 shows the results obtained for 40 fibres, for which both the mean diameter before the tensile test (average of the measurements made on 5 optical micrographs) and the diameter near the rupture point after the tensile test (measured on a SEM micrograph) were determined. These two diameters were used to calculate the corresponding Young's modulus. First it can be seen that there is no relationship between the failure point and the mean diameter: the fibre did not fail where its diameter was the smallest (weakest point) or the largest (on a defect), which would have brought about a significant shift towards lower or higher diameter values respectively. The average diameters calculated for these 40 fibres and obtained either by averaging optical micrograph measurements ("mean diameter") or by measuring the fibre dimension near the rupture plane ("failure diameter") are 19 ± 5 μm and 18 ± 4 μm respectively. Secondly, it appears that the slope of the Young's modulus-fibre diameter graph, negative when plotted as a function of mean fibre diameter, is almost horizontal when plotted as a function of failure diameter. In this case, the modulus reflects correctly the stiffness of the material and can be estimated at 56 GPa (rather than 51 GPa obtained with the mean diameter). Nevertheless, whatever the calculation method used, the standard deviation around the mean Young's modulus value remains as high as 17 GPa.

This relatively high value of Young's modulus has to be compared with that of E-glass fibres (about 74 GPa). When dealing with the specific properties of these two kinds of fibres, flax appears globally more rigid than glass: as the flax and glass densities are about 1.4 and 2.5 respectively, the specific Young's modulus reaches 40 GPa for flax fibres and 29 GPa for glass fibres. This justifies the interest of flax as a reinforcement for composites instead of E-glass fibres: theoretically, the rigidity is likely to be higher in the case of eco-composites than in the case of synthetic composites, for the same composite weight. Nevertheless, in practice, this is rarely true (Madsen & Lilholt, 2003; Wambua, Ivens, & Verpoest, 2003).

3.4. Internal structure of flax fibres

Using the FIB microscope, the strong interaction between the flax fibre and the gallium ion beam enables the inner structure of the fibre to be represented in a different way from what is commonly done with a SEM or a TEM. Indeed, the beam literally destroys the fibre; thus, the contrast obtained on the FIB images reveals the Ga^+ sensitivity of the different parts of the fibre, allowing the localization of soft or stiff polymers, or of badly- or well-organized structures (Domengès & Charlet, 2010).

One of the main results obtained from these experiments is the distinction of several layers on an elementary fibre cross-section (Fig. 9): an external 0.6 μm thick Ga^+ insensitive layer (white arrow in Fig. 9c), a uniform highly sensitive intermediate layer of several micrometers of thickness, and a 3–4 μm thick internal layer made of 4 concentric lamellae spaced by highly Ga^+ sensitive interfaces (white arrows in Fig. 9b). This organisation, revealed from the observation of several elementary flax fibres, is quite different from the usual description of a flax fibre (cf. Fig. 1) (Forgacs, 1963; Harada, Miyazaki, & Wakashima, 1958; Wardrop & Bland, 1959). Some TEM micrographs had already shown the presence of concentric layers around the lumen (Morvan et al., 2003), but their thickness compared to the fibre size was much lower than that highlighted by the FIB method. A new schematic representation of the fibre structure, based on these new results, is given in Fig. 10.

For the moment, mainly because of the small size of the sample, no information on the chemical composition or the cellulosic organisation in each layer is available to help in comparing the old and new representations of the elementary flax fibre. That is to say, for example concerning the 4 inner layers, that they may be identical in structure and thus all correspond to the old S3 cell wall, or they may be intermediate layers between the S3 and the S2 layers and exhibit a different organisation of their cellulose microfibrils. Further experiments must be carried out on a FIB device to determine the microfibrilar structure of each layer.

Nevertheless, this concentric multi-layer model suggests delamination as a possible mode of rupture of the elementary fibre, as already proposed by Baley (2002), in addition to the common straight failure which leads to a "smooth" aspect of the rupture plane, as attested by the images presented in Fig. 11.

4. Conclusion

Investigations were carried out on flax fibres at different levels of observation. New structural information was obtained and correlated with mechanical properties. The correct understanding of fibre deformation under mechanical stress is an issue for the comparison of flax fibres with other natural fibres and the simulation of the behaviour of derived flax fibre-based composite materials.

At the stem level, the variation in mean fibre diameter as a function of the fibre position along the stem (from 30 μm for bottom fibres until 18 μm for middle and top fibres) was studied. The results underline the fact that fibres taken near the root are the widest of the stem.

On a smaller scale, intra-bundle size variability (i.e. size variation along a single bundle) as well as inter-fibre size scattering (i.e. calculated from several fibre cross-sections) were proved to be linked to the large intra-fibre size dispersion, as highlighted by SEM experiments. Concerning the mechanical properties, it was shown that the technical fibres (i.e. parts of bundles) useable in composites should be of medium size, that is to say not too large to avoid elementary fibre sliding and not too small to limit the extraction processes and the resulting damage. Moreover, because of the large fibre width scattering, a new method for the calculation of mechanical properties, based on the diameter measured near the fibre rupture plane rather than on the commonly used mean fibre diameter, was proposed and validated.

Lastly, FIB experiments have enabled a new schema of the fibre's internal structure to be drawn, in which the different cell wall thicknesses notably differ from the classical representation. This data will soon be completed by finer synchrotron analysis, which would enable the fibre structure to be correctly modelled.

Acknowledgments

The authors are grateful to the "Réseau Inter-Régional 'Matériaux Polymères, Plasturgie' du Grand Bassin Sud-Parisien" for its financial support, as well as to Dr. Bernadette Domengès (LAMIPS,

Caen, France) and Dr. Laurent Bizet (LOMC, Le Havre, France) for their participation in the experiments and discussions.

References

Andersons, J., Sparnins, E., Joffe, R., & Wallström, L. (2005). Strength distribution of elementary flax fibres. *Composites Science and Technology*, *65*, 693–702.

Baley, C. (2002). Analysis of the flax fibers tensile behaviour and analysis of the tensile stiffness increase. *Composites: Part A*, *33*, 939–948.

Batra, S. K. (1998). Other long vegetable fibers. In M. Lewin, & E. M. Pearce (Eds.), *Handbook of fiber chemistry* (pp. 505–575). New York, USA: Marcel Dekker.

Beukers, A., & Van Hinte, E. (1999). *Lightness: The inevitable renaissance of minimum energy structures*. Rotterdam, The Netherlands: O10 Publishers.

Bos, H.L. (2004). The potential of flax fibres as reinforcement for composite materials. *PhD thesis*. University of Eindhoven, The Netherlands.

Bos, H. L., Van den Oever, M. J. A., & Peters, O. C. J. J. (2002). Tensile and compressive properties of flax fibres for natural fibre reinforced composites. *Journal of Materials Science*, *37*, 1683–1692.

Bossuyt, V. (1941). Etude la structure et des propriétés mécaniques de la fibre de lin. *PhD thesis*. University of Lille, France.

Charlet, K. (2008). Contribution à l'étude de composites unidirectionnels renforcés par des fibres de lin – Relation entre la microstructure de la fibre et ses propriétés mécaniques. *PhD thesis*. University of Caen, France.

Charlet, K., Morvan, C., Bréard, J., Jernot, J. P., & Gomina, M. (2006). Etude morphologique d'un composite naturel – la fibre de lin. *Revue des Composites et des Matériaux Avancés*, *16*, 11–24.

Davies, G. C., & Bruce, D. M. (1998). Effect of environmental relative humidity and damage on the tensile properties of flax and nettle fibres. *Textile Research Journal*, *68*, 623–629.

Domengès, B., & Charlet, K. (2010). Direct insights on flax fiber structure by focused ion beam microscopy. *Journal of Microscopy and Microanalysis*, *16*, 175–182.

Eichhorn, S. J., Baillie, C. A., Zafeiropoulos, N., Mwaikambo, L. Y., Ansell, M. P., Dufresne, A., et al. (2001). Current international research into cellulosic fibres and composites. *Journal of Materials Science*, *36*, 2107–2131.

Fink, H. P., Hofmann, D., & Purz, H. J. (1990). On the fibrillar structure of native cellulose. *Acta Polymerica*, *41*, 131–137.

Forgacs, O. L. (1963). The characterization of mechanical pulps. *Pulp Paper Magazine Canada*, *64*, T89–T118.

Fujita, M., & Harada, H. (1991). Ultrastructure and formation of wood cell wall. In D. N. S. Hon, & N. Shiraishi (Eds.), *Wood and cellulosic chemistry* (pp. 3–57). New York, USA: Marcel Dekker.

Ganster, J., & Fink, H. P. (1999). Physical constants of cellulose. In J. Brandrup, E. H. Immergut, & E. A. Grulke (Eds.), *Polymer handbook*. New York, USA: Wiley.

Harada, H., Miyazaki, Y., & Wakashima, T. (1958). Electron-microscopic investigation on the cell wall structure of wood. *Bulletin of Forest Experimental Station (Meguro, Tokyo, Japan)*, *104*, 1–115.

Hearle, J. W. S. (1962). The structure and mechanical properties of fibres. *Journal of Textile Institute Proceedings*, *53*, 449–464.

Madsen, B., & Lilholt, H. (2003). Physical and mechanical properties of unidirectional plant fibre composites – an evaluation of the influence of porosity. *Composite Science and Technology*, *63*, 1265–1272.

Morvan, C., Andème-Onzighi, C., Girault, R., Himmelsbach, D. S., Driouich, A., & Akin, D. E. (2003). Building flax fibres: More than one brick in the walls. *Plant Physiology and Biochemistry*, *41*, 935–944.

Näslund, P., Vuong, R., Chanzy, H., & Jésior, J. C. (1988). Diffraction contrast transmission electron microscopy on flax fiber ultrathin cross-sections. *Textile Research Journal*, *58*, 414–417.

Romhány, G., Karger-Kocsis, J., & Czigány, T. (2003). Tensile fracture and failure behavior of technical flax fibers. *Journal of Applied Polymer Science*, *90*, 3638–3645.

Rowell, R. M., Han, J. S., & Rowell, J. S. (2000). Characterization and factors effecting fiber properties. In E. Frollini, A. L. Leao, & L. H. C. Mattoso (Eds.), *Natural polymers and agrofibers composites* (pp. 115–134). Brazil: San Carlos.

Sakurada, I., Nukushina, Y., & Ito, T. (1962). Experimental determination of the elastic modulus of crystalline regions in oriented polymers. *Journal of Polymer Science*, *57*, 651–660.

Troger, F., Wegener, G., & Seemann, C. (1998). Miscanthus and flax as raw material for reinforced particleboards. *Industrial Crops and Products*, *8*, 113–121.

Van den Oever, M. J. A., Bos, H. L., & Van Kemenade, M. J. J. M. (2000). Influence of the physical structure on the mechanical properties of flax fibre reinforced polypropylene composites. *Applied Composite Materials*, *7*, 387–402.

Wambua, P., Ivens, J., & Verpoest, I. (2003). Natural fibres: Can they replace glass in fibre reinforced composites? *Composite Science and Technology*, *63*, 1259–1264.

Wardrop, A. B., & Bland, D. E. (1959). The process of lignification in woody plants. In *Proceedings of the 4th international conference of biochemistry* (pp. 76–81). New York, USA: Pergamon Press.

Weightman, R., & Kindred, D. (2005). Review and analysis of breeding and regulation of hemp and flax varieties available for growing in the UK. *Final report for the Department for Environment Food and Rural affairs*, ADAS UK Ltd.

Zafeiropoulos, N. E., & Baillie, C. A. (2007). A study of the effect of surface treatments on the tensile strength of flax fibres. Part II. Application of Weibull statistics. *Composites: Part A*, *38*, 629–638.